metals

MDPI

Article

Effect of Aging Process on the Strain Rate Sensitivity in V-Containing TWIP Steel

Shaoheng Sun and Zhiyong Xue *

Institute of Advanced Materials, North China Electric Power University, Beijing 102206, China; sunsh@ncepu.edu.cn

* Correspondence: xuezy@ncepu.edu.cn

Abstract: The dynamic tensile behavior of the twinning-induced plasticity (TWIP) steel with the vanadium carbide is investigated at different strain rates of 10^{-4}, 10^{-3}, 10^{-2} and 0.05 s^{-1}. Microstructure characterization, carried out using back scatter electron diffraction (EBSD) and transmission electron microscopy (TEM), shows a homogeneous face center cubic structured matrix with uniformly dispersed vanadium carbide. The vanadium carbide is controlled by the aging temperature and time. The best comprehensive mechanical properties are achieved when the tested steel is aged at 550 °C for 5 h. With the increase of strain rate, the tensile strength and work hardening rate decrease, and the tested material shows negative strain rate sensitivity. This would be due to an increase in stacking fault energy caused by temperature rise by adiabatic heating, which must suppress the formation of twinning. On the other hand, the strain rate sensitivity is affected by dynamic strain aging (DSA). With the increase of strain rate, the DSA weakens, which causes negative strain rate sensitivity. The tensile strength and strain rate sensitivity value both increase first and then decrease with the increase of vanadium carbide size. This is because the tensile strength is mainly affected by the vanadium carbide. In addition to the vanadium carbide, the strain rate sensitivity is also affected by the amount of solute atom (V and C) during the dynamic strain aging process.

Keywords: TWIP steel; vanadium carbide; aging process; strain rate sensitivity

Citation: Sun, S.; Xue, Z. Effect of Aging Process on the Strain Rate Sensitivity in V-Containing TWIP Steel. *Metals* **2021**, *11*, 126. https://doi.org/10.3390/met11010126

Received: 10 December 2020
Accepted: 7 January 2021
Published: 10 January 2021

1. Introduction

In recent years, the development of new advanced high strength steels (AHSS) has drawn more and more attention for reducing vehicle weight and oil consumption in the automobile industries due to the deteriorating environment [1,2]. Among the AHSS, high manganese twinning-induced plasticity (TWIP) steel is considered to be a promising candidate for high strength and excellent plasticity [3]. The application of TWIP steel is limited because of the relatively low yield strength. In order to increase the yield strength, the commonly employed approaches include precipitation strengthening with micro-alloying additions [4], grain refinement [5] and pre-straining [6]. Among the micro-alloy, vanadium (V) is the most commonly used in steel to achieve precipitation hardening [7–9]. The vanadium carbide is well known as an excellent method for increasing strength in TWIP steels [4]. However, the strength, especially the tensile strength, is significantly affected by the strain rate. During crash of the vehicle, the strain rate encompasses a wide range. Some studies have reported that the high-Mn steel has a negative strain rate sensitivity and the tensile strength decreases with the rise of strain rate [10,11]. Hence, the strain rate sensitivity of TWIP steel is very important for the vehicle safety. The strain rate sensitivity is affected by the microstructure, such as grain size [12]. Whereas extensive research has been focused on the deformation behavior of TWIP steel, there are only a few reports regarding a detailed analysis of the dynamic strain aging (DSA) on the strain rate sensitivity. In particular, studies on the effect of vanadium carbide's size on the strain rate sensitivity have not yet been carried out. The objective of this work is to elucidate the effect of vanadium carbides on the strain rate sensitivity in a vanadium-containing TWIP

steel. The vanadium carbides are obtained through aging annealing treatment. The strain rate sensitivity is investigated by tensile test at different strain rates, 10^{-4}, 10^{-3}, 10^{-2} and 5×10^{-2} s^{-1}.

2. Experimental Procedure

The chemical composition of the tested alloy is: Fe-17.1Mn-0.34C-0.76V-0.26Si -0.81Al-0.006P-0.011S (in mass%). After vacuum melting, the ingot was forged and then homogenized at 1180 °C for 1.5 h. The bulks were hot-rolled in the temperature range of 900–1100 °C, and the final thickness was 4 mm. Subsequently, the sheets were heated at 1080 °C for 10 min, and then quenched by water. In order to study the effect of aging temperature, the tested materials were aged for 5 h at different temperatures, 450, 550, 650 and 750 °C. Analogously, in order to study the effect of aging time, the tested materials were aged at 550 °C for 1, 2, 5, and 10 h. The tensile specimens were cut from the sheet parallel to the rolling direction and the oxide layer was removed. The tensile tests were performed at room temperature on an electronmechanical universal testing machine (CMT5205, MTS Systems (China) Co., Ltd., Shanghai, China) with a load capacity of 200 kN. Tensile test plate sample is shown in Figure 1 (the unit is mm), and the gauge length was 50 mm. The employed strain rates were 10^{-4}, 10^{-3}, 10^{-2} and 5×10^{-2} s^{-1}, respectively. For the detailed analysis of the microstructures, the tested sample was characterized by a field emission scanning electron microscope FEI-450 (FEI Company, Hillsboro, OR, USA), equipped with back scatter electron diffraction (EBSD) unit. The step size was 0.2 μm. The accelerating voltage was 20 kV. The vanadium carbide was characterized by transmission electron microscopy (TEM), FEI Tecnai F20 (Hillsboro, OR, USA). The samples for TEM observation were prepared by double-jet thinning in the electrolyte of 5% perchloric acid and 95% glacial acetic acid (University of Science and Technology Beijing, Beijing, China).

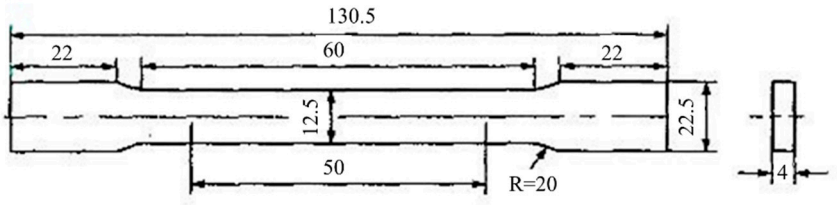

Figure 1. Drawing of the tensile test sample; the unit is mm.

3. Results

3.1. Microstructure Change before and after Aging Process

Figure 2 shows the microstructure of the hot-rolled and quenched alloy studied in the present research. The grain size distributions are homogeneous. Moreover, a large fraction of annealing twins was observed in most of the grains in the alloy. The average grain size was about 12 μm.

The vanadium carbides formed during the aging treatment with different temperatures in the tested steel are shown in Figure 3. It can be concluded that the diameter of the carbide increases with the rise of aging temperature [13]. The qualitative chemical composition of the carbide has been confirmed to contain a certain content of vanadium by using Nano Probe energy-dispersion X-ray spectra (EDS), as shown in Figure 3e. The chemical composition of the vanadium carbides is listed in Table 1.

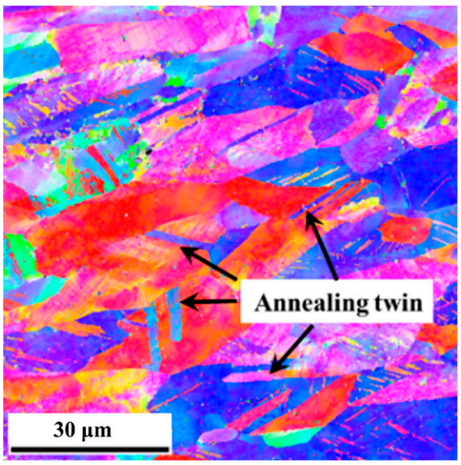

Figure 2. Microstructure of the tested alloy.

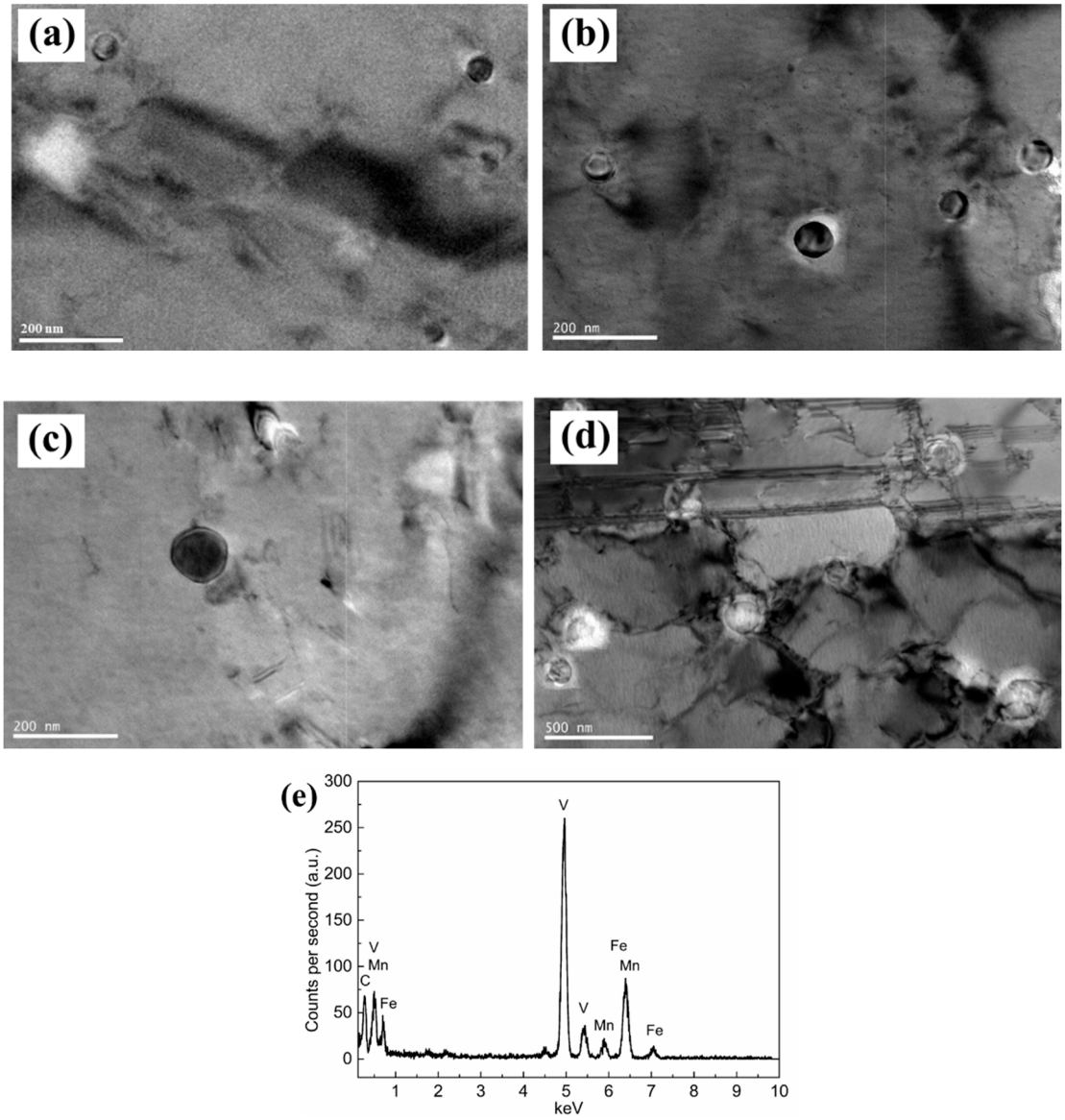

Figure 3. Transmission electron microscopy (TEM) micrograph showing the distribution of carbides aged at different temperatures: (**a**) 450 °C, (**b**) 550 °C, (**c**) 650 °C, (**d**) 750 °C, (**e**) X-ray energy-dispersion spectra (EDS) of the carbides.

Table 1. The chemical composition of the vanadium carbides.

Elements	C	V	Mn	Fe	Total
wt.%	12.11	61.28	4.28	22.33	100
at.%	37.50	44.74	2.90	14.87	100

The microstructure of the vanadium carbides formed under different aging times at 550 °C is shown in Figure 4. It can be confirmed that the diameter of the carbide increases with the increase of aging time.

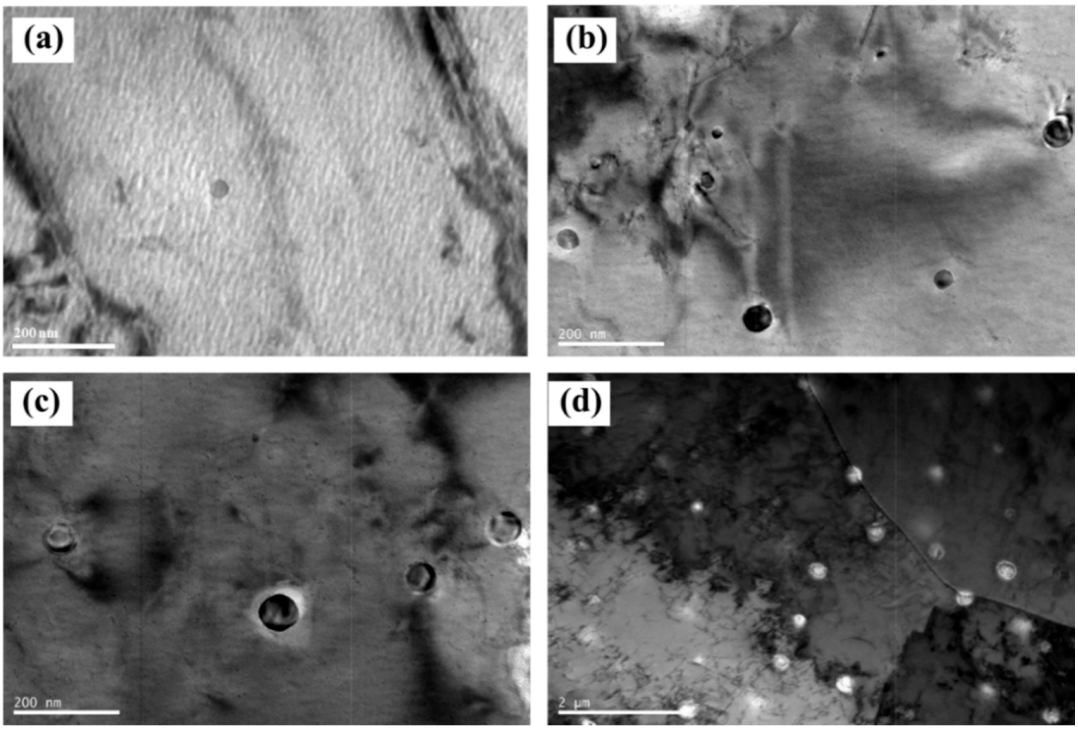

Figure 4. TEM micrograph showing the distribution of carbides aged at different holding times: (**a**) 1 h, (**b**) 2 h, (**c**) 5 h and (**d**) 10 h.

3.2. Effect of Aging Process on Tensile Behavior

Figure 5 shows the engineering stress–strain curve (a) and the work hardening curve (b) of the as-aged samples with different aging temperatures. The work hardening curve is calculated as the first derivative of the true stress to the true strain. With the rise of the aging temperature, the yield strength and tensile strength first exhibit increase and then decrease, while the total elongation consistently decreases. Especially when the aging temperature increases to 650 °C, the total elongation declines rapidly. The safety criterion of the vehicle is based not only on the tensile strength but also the elongation. High production of strength and elongation indicates that more energy could be absorbed by the material during a crash. Hence, the comprehensive mechanical performance is the best when the aging temperature is 550 °C. The evolution trends of the work hardening rate at different aging temperatures are similar, and the curves exhibit three different regimes, as shown in Figure 3b. Firstly, the work hardening rates decrease continuously and rapidly. With further increase of the strain, the curves decrease slowly until the samples fracture. The work hardening rate has a slight rise with the increase of the aging temperature. It can also be concluded that the Portevin–Le Chatelier (PLC) effect weakens with the rise of aging temperature, which is due to the growth of the vanadium carbides resulting in the decrease of solid solution carbon [14].

Figure 6 shows the engineering stress–strain curves (a) and the corresponding work hardening curves (b) of the as-aged samples with various aging times at 550 °C. With the increase of aging time, the yield strength and tensile strength show first increased and then decreased trend. When the aging time prolongs to 5 h, the tensile strength and work hardening rate achieve the highest value.

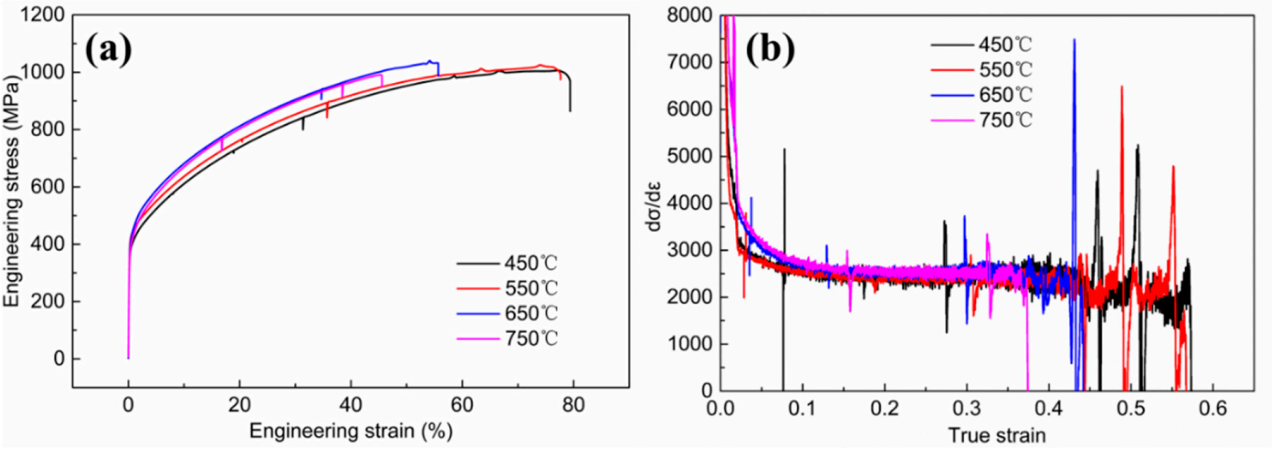

Figure 5. Mechanical properties of the tested alloy demonstrated in terms of the engineering stress–strain curve (**a**) and the corresponding work hardening curve with respect to true strain (**b**).

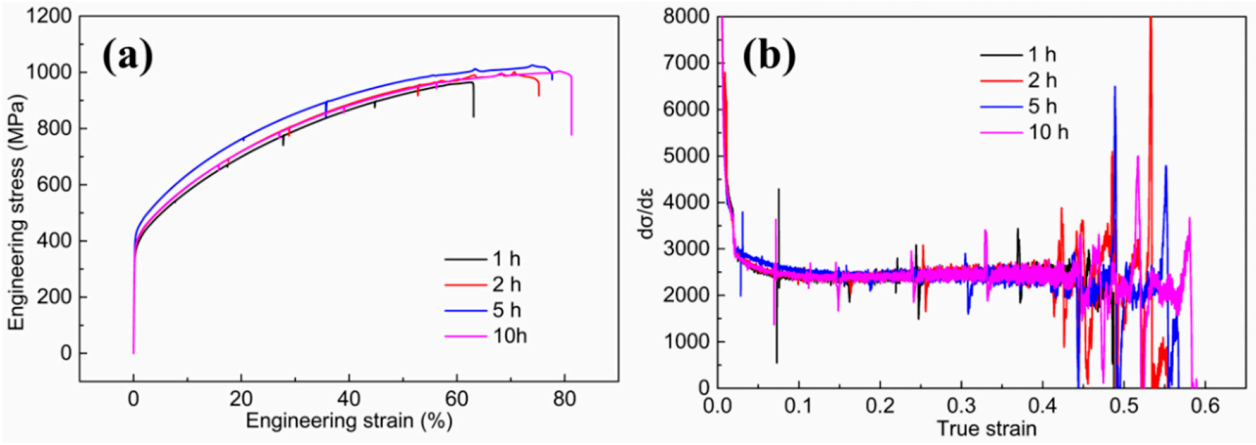

Figure 6. Mechanical properties of the tested alloy demonstrated in terms of the engineering stress–strain curves (**a**) and the corresponding work hardening curves with respect to true strain (**b**).

3.3. Effect of Strain Rate on Tensile Behavior

The mechanical properties under different strain rates with different aging temperatures are shown in Figure 7, which are the engineering stress–engineering strain curves and the corresponding work hardening curves. The result shows that all the tensile strengths and work hardening rates of the tested steel aged at different temperatures decrease with the rise of strain rate. The PLC effect weakens with the rise of strain rate, which is due to the increase of critical strain of the PLC effect [14].

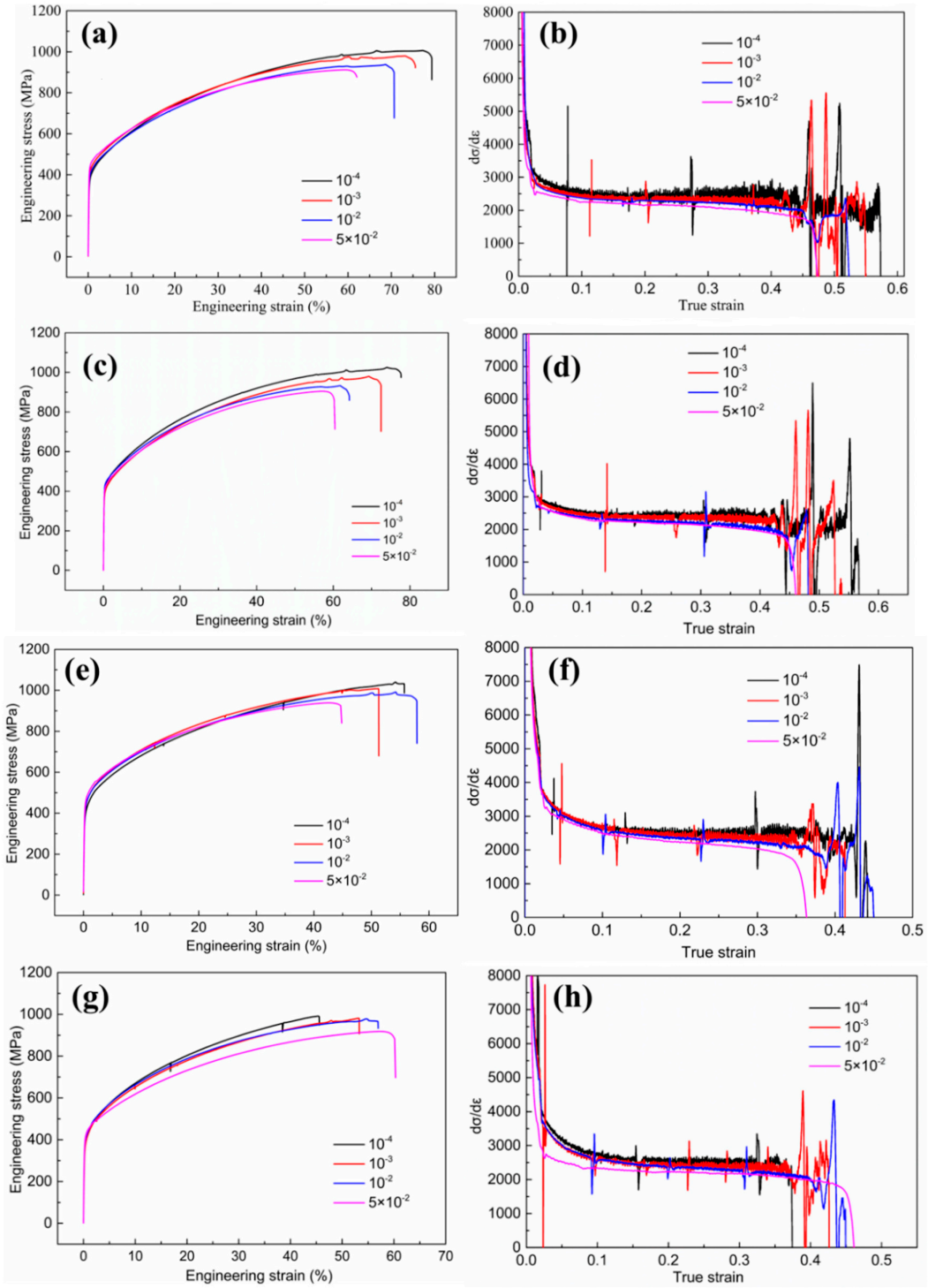

Figure 7. The engineering stress-engineering strain curves and corresponding work hardening rate-true curves of the tested material at different strain rates. (**a**,**b**) 450 °C, (**c**,**d**) 550 °C, (**e**,**f**) 650 °C, (**g**,**h**) 750 °C.

The mechanical properties under different strain rates at different aging times are shown in Figure 8. Figure 8a,c,e,g are the engineering stress-engineering strain curves and Figure 8b,d,f,h are the corresponding work hardening curves. The result shows that all the tensile strength and work hardening rate of the tested steel decrease with the rise of strain rate.

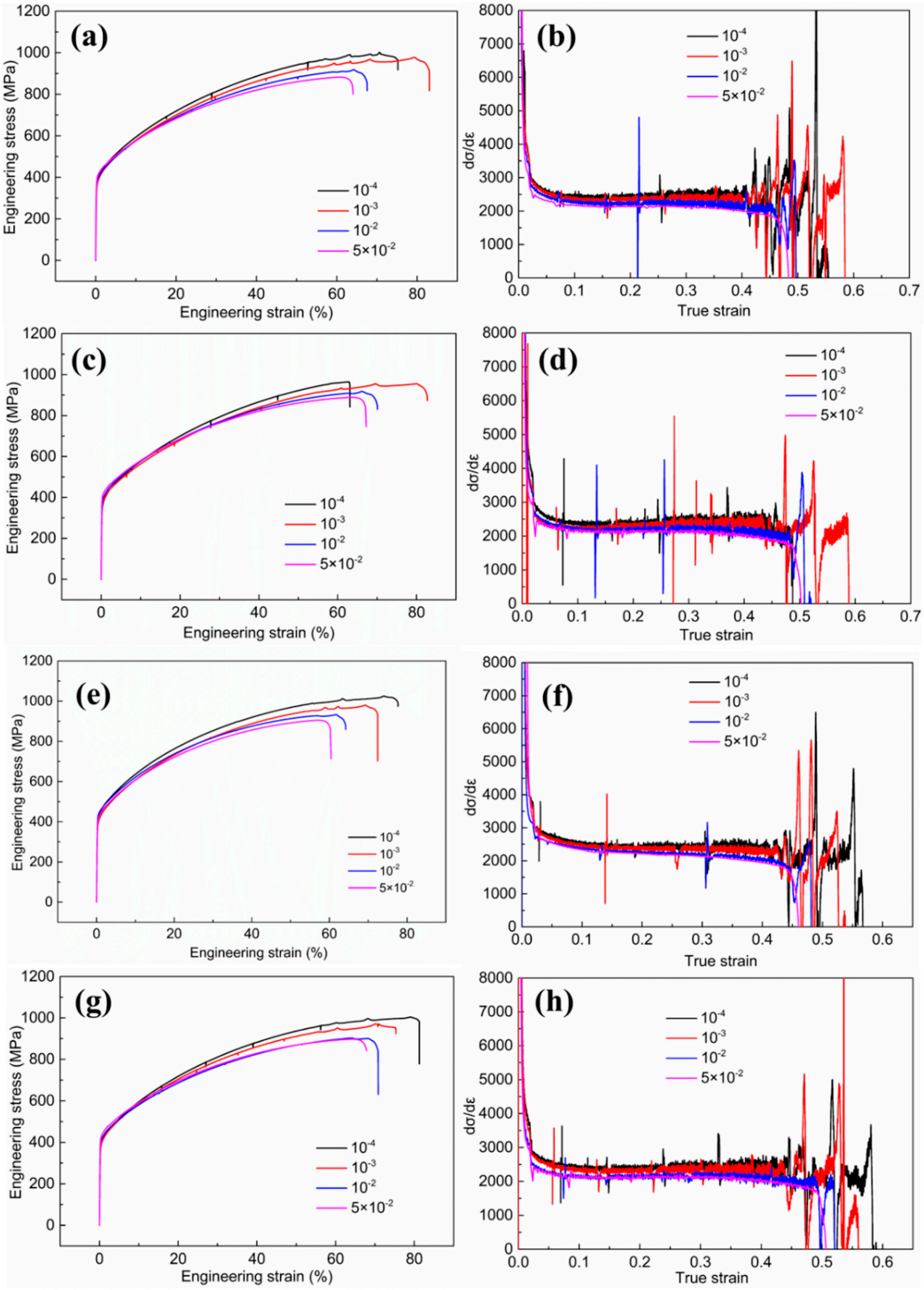

Figure 8. The engineering stress-engineering strain curves and corresponding work hardening rate-true curves of the tested material at different strain rates. (**a**,**b**) 1 h, (**c**,**d**) 2 h, (**e**,**f**) 5 h, (**g**,**h**) 10 h.

4. Discussion

4.1. Aging Strengthening

The vanadium carbides are usually considered as hard phase. During the plastic deformation process, dislocation cannot shear the vanadium carbides. The vanadium carbides will be bypassed by dislocation and dislocation loops will appear around the vanadium carbides, which is called Orowan mechanism [7]. With the increase of deformation degree, the dislocation loops are continuously stored and the work hardening rate

increases. As the aging time prolongs, the nano-sized vanadium carbides gradually grow up and the strength of the material increases. When the aging time is further increased, the over-aging occurs, which results in the formation of large-size vanadium carbides, and thus, the strength is reduced [15,16].

4.2. Strain Rate Sensitivity

The tensile strengths under different strain rates are listed in Table 2. The strain rate sensitivity value m can be defined by [17]:

$$m = \frac{d\ln\sigma}{d\ln\dot{\varepsilon}} \quad (1)$$

where σ and $\dot{\varepsilon}$ represent the tensile strength and strain rate, respectively. As shown in Table 3, the strain rate sensitivity values at different aging temperatures are all negative, and the value increases first and then decreases with the increase of aging temperature. The negative value suggests that the mechanical property of the tested material becomes worse during deformation with increase of strain rate. Tensile strength reaches the highest value when aged at 650 °C. Whereas the strain rate sensitivity value reaches the highest value when aged at 550 °C.

Table 2. The tensile strength of the tested steel at different strain rates (MPa).

Strain Rate	450 °C	550 °C	650 °C	750° C
10^{-4}	1006 ± 17	1025 ± 14	1040 ± 18	991 ± 15
10^{-3}	980 ± 14	980 ± 26	1008 ± 13	981 ± 12
10^{-2}	938 ± 21	933 ± 22	991 ± 21	978 ± 27
0.05	912 ± 11	905 ± 14	939 ± 16	918 ± 23

Table 3. The strain rate sensitivity value at different aging temperatures.

Temperature	450 °C	550 °C	650 °C	750 °C
m	−0.0161	−0.0202	−0.0151	−0.0105

The tensile strength of the tested steel at different strain rates aged at 550 °C for different times are listed in Table 4. The strain rate sensitivity values at different aging times are shown in Table 5 and all present negative. The value increases first and then decreases with the increase of aging time. Tensile strength reaches the highest value when aged at 550 °C for 5 h. Whereas the strain rate sensitivity value reaches the highest value when aged at 550 °C for 2 h. It is interesting that the strain rate sensitivity under different aging temperatures and times both precede the tensile strength accessing peak with the increase of aging temperature and time, which means that the strain rate sensitivity can act as an indication for the optimum aging process.

Table 4. The tensile strength of the tested steel under different strain rates (MPa).

Strain Rate	1 h	2 h	5 h	10 h
10^{-4}	964 ± 14	1002 ± 11	1025 ± 14	1004 ± 16
10^{-3}	955 ± 20	977 ± 24	980 ± 26	971 ± 14
10^{-2}	918 ± 18	918 ± 16	933 ± 22	902 ± 21
0.05	889 ± 16	882 ± 21	905 ± 14	897 ± 15

In addition to the negative strain rate sensitivity, the high strain rate leads to a negative work hardening rate sensitivity. The relationship between the work hardening rate sensitivity and strain rate sensitivity parameters can be defined by [18]:

$$m' = m + \frac{\sigma}{\frac{d\sigma}{d\varepsilon}} \frac{\partial m}{\partial \varepsilon} \quad (2)$$

Because of $\sigma > 0$, $\frac{d\sigma}{d\varepsilon} > 0$ and $\frac{\partial m}{\partial \varepsilon} < 0$, m' is more negative than m, which indicates that the ability of work hardening rate becomes weakened with the increase of strain rate.

Table 5. The strain rate sensitivity value at different aging times.

Time	1 h	2 h	5 h	10 h
m	−0.0133	−0.0211	−0.0202	−0.0199

4.3. Adiabatic Heating

The negative work hardening rate sensitivity and strain rate sensitivity are obtained because of the adiabatic heating at a high strain rate. The adiabatic temperature rise can be shown as follows [19,20]:

$$\Delta T = \frac{\Delta Q}{\rho C_p} = \frac{\beta}{\rho C_p} \int_{\varepsilon_1}^{\varepsilon_2} \sigma d\varepsilon \quad (3)$$

where β is the coefficient of heat conversion from plastic work to heat, ρ is the density of the tested alloy, C_p is the typical specific heat capacity. The vast amounts of heat energy generated during the plastic deformation will build up because there is not enough time to escape at high strain rate. The ΔT value of the sample surface increases from 39.87 to 59.85 °C when the strain rate increases from 1×10^{-4} to 1×10^{-1} s^{-1} [11]. It has been widely agreed that the deformation heat can cause the increase of stacking fault energy (SFE). The value of SFE would increase with increasing strain rate. The stacking fault energy (SFE) plays a key role in determining the deformation mechanisms of TWIP steel. Hence, the TWIP effect is restrained at high strain rate. The inhibiting effect of the twin on the dislocations would weaken. The tensile strength and work hardening rate decrease consequently.

4.4. Dynamic Strain Aging (DSA)

The high work hardening rate of the TWIP steel is due to not only twin but also to dynamic strain aging [21]. In addition to the adiabatic heating, dynamic strain aging (DSA) has a great influence on the strain rate sensitivity. DSA is determined by the velocity of solute atom diffusion relative to the dislocation velocity [22]. A solute atmosphere will be formed around a moving dislocation in a solid solution, which will act as strong obstacles to the dislocation motion, thus leading to strain hardening. During the plastic deformation process, when the dislocation velocity is larger than the velocity of solute atom diffusion, the DSA will occur. DSA is a strengthening phenomenon in metals and alloys.

With the increase of strain rate, the velocity of the mobile dislocation increases, the time for DSA decreases, and the pinning effect for mobile dislocation diminishes. Therefore, the tensile strength decreases with the rise of strain rate, and the material shows a negative strain rate sensitivity, which corresponds with the weakened PLC effect. Though the DSA has developed earlier, the effect of the second phase particle on the DSA has rarely been reported.

Solid solubility product formula of V and C atom in FCC matrix can be shown as follows [15]:

$$\lg\{[V] \times [C]\} = 6.72 - \frac{9500}{T} \quad (4)$$

where [V] and [C] are the mass fraction of V and C dissolved in the matrix, respectively. T is the aging temperature, K. The rate of V and C atom diffusion in FCC matrix can be shown as follows [15]:

$$D_C = 0.1 \exp\left(-\frac{136,000}{RT}\right) \quad (5)$$

$$D_V = 0.28 \exp\left(-\frac{264,000}{RT}\right) \quad (6)$$

where R is the gas constant, and T is the aging temperature, K.

When the tested material is aged at 450 °C, atom diffusion velocity is low. Though the precipitation driving force of vanadium carbide is very high, a large number of solute atoms are dissolved in the matrix as a solid solution. With the rise of aging temperature, atom diffusion velocity quickens, which causes the increase of the vanadium carbide size. Thereupon, the number of solute atoms decreases, the DSA effect weakens, and the strain rate sensitivity value decreases. With the further increases of aging temperature, precipitation driving force will be reduced. The number of solute atoms increases, and can be enhanced. Hence, the strain rate sensitivity value increases.

When aged at 550 °C, the number of solute atoms decreases with the increase of aging time, and the DSA effect weakens, which causes the decrease of strain rate sensitivity value. However, with the further increases of aging time, the size of the vanadium carbide continues to increase. On the one hand, the amount of vanadium carbide drops, which results in the number of obstacles to the dislocation motion decreasing. The dislocation velocity decreases. On the other hand, with the vanadium carbide coarsening, the interface between vanadium carbide and matrix will transform into incoherent interface, and a large number of vacancies can be absorbed by the interface, which causes the decrease of vacancy concentration [23–25]. Thereupon, the velocity of solute atom diffusion decreases and the velocity difference between the solute atom diffusion and the dislocation will increase, which can reinforce the DSA effect. Therefore, the strain rate sensitivity value increases.

5. Conclusions

In summary, the effect of vanadium carbide on the strain rate sensitivity in TWIP steel is proposed by controlling the aging process. The size of the vanadium carbide increases with the rise of aging temperature and time. The best comprehensive mechanical properties are achieved when the tested steel is aged at 550 °C for 5 h. With the increase of strain rate, the tensile strength decreases and the tested material shows negative strain rate sensitivity, which is because of not only the adiabatic heating, but also the dynamic strain aging. The adiabatic heating will cause an increase in stacking fault energy, which must suppress the formation of twinning. The dynamic strain aging (DSA) weakens at high strain rate. The DSA is affected by the vanadium carbide. With the increase of vanadium carbide size, the strain rate sensitivity value first rises and then falls.

Author Contributions: Conceptualization: S.S.; methodology: S.S.; resources: S.S. and Z.X.; writing—original draft preparation: S.S.; writing—review and editing: S.S.; project administration: Z.X. All authors have read and agreed to the published version of the manuscript.

Funding: This work was supported by the Fundamental Research Funds for the Central Universities (2020MS058).

Institutional Review Board Statement: Not applicable.

Informed Consent Statement: Not applicable.

Data Availability Statement: Not applicable.

Conflicts of Interest: The authors declare no conflict of interest.

References

1. Sun, B.; Krieger, W.; Rohwerder, M.; Ponge, D.; Raabe, D. Dependence of hydrogen embrittlement mechanisms on microstructure-Driven hydrogen distribution in medium Mn steels. *Acta Mater.* **2020**, *183*, 313–328. [CrossRef]
2. Sun, B.; Palanisamy, D.; Ponge, D.; Gault, B.; Fazeli, F.; Scott, C.; Yue, S.; Raabe, D. Revealing fracture mechanisms of medium manganese steels with and without delta-Ferrite. *Acta Mater.* **2019**, *164*, 683–696. [CrossRef]
3. Cooman, B.C.D.; Estrin, Y.; Kim, S.K. Twinning-Induced plasticity (TWIP) steels. *Acta Mater.* **2018**, *142*, 283–362. [CrossRef]
4. Scott, C.; Remy, B.; Collet, J.-L.; Cael, A.; Bao, C.; Danoix, F.; Malard, B.; Curfs, C. Precipitation strengthening in high manganese austenitic TWIP steels. *Int. J. Mater. Res.* **2011**, *102*, 538–549. [CrossRef]

5. Kang, S.; Jung, J.; Kang, M.; Woo, W.; Lee, Y. The effects of grain size on yielding, strain hardening, and mechanical twinning in Fe–18Mn–0.6C–1.5Al twinning-Induced plasticity steel. *Mater. Sci. Eng. A* **2016**, *652*, 212–220. [CrossRef]
6. Hamada, A.S.; Järvenpää, A.; Honkanen, M.; Jaskari, M.; Porter, D.A.; Karjalainen, L.P. Effects of Cyclic Pre-Straining on Mechanical Properties of an Austenitic Microalloyed High-Mn Twinning-Induced Plasticity Steel. *Procedia Eng.* **2014**, *74*, 47–52. [CrossRef]
7. Yen, H.; Huang, M.; Scott, C.P.; Yang, J. Interactions between deformation-Induced defects and carbides in a vanadium-CONTAINING TWIP steel. *Scr. Mater.* **2012**, *66*, 1018–1023. [CrossRef]
8. Chateau, J.P.; Dumay, A.; Allain, S.; Jacques, A. Precipitation hardening of a FeMnC TWIP steel by vanadium carbides. *J. Phys. Conf. Ser.* **2010**, *240*, 12023. [CrossRef]
9. Kwon, Y.A.; Zargaran, A.A.; Ryu, J.H.A.; Kim, N.J.A.N. Effect of annealing conditions on the microstructure and tensile properties of 0.5 V containing Fe-16Mn-0.8C-0.5Si steel. *Scr. Mater.* **2019**, *172*, 125–129. [CrossRef]
10. Sun, S.; Zhao, A.A.Z.U.; Wu, Q. Effect of strain rate on the work-Hardening rate in high-Mn steel. *Mater. Sci. Technol.* **2017**, *33*, 1306–1311. [CrossRef]
11. Xu, M.; Mi, Z.; Li, H.; Tang, D.; Jiang, H. Deformation mechanism transition in Fe–17Mn–0.4C–0.06V TWIP steel with different strain rates. *Mater. Sci. Technol.* **2018**, *34*, 242–251. [CrossRef]
12. Yin, F.; Hu, S.; Xu, R.; Han, X.; Qian, D.; Wei, W.; Hua, L.; Zhao, K. Strain rate sensitivity of the ultrastrong gradient nanocrystalline 316L stainless steel and its rate-Dependent modeling at nanoscale. *Int. J. Plast.* **2020**, *129*, 102696. [CrossRef]
13. Zeng, J.; Chen, C.; Wang, J.; Ren, Z.; Shi, W. Effect of annealing treatment on the microstructure and mechanical properties of Fe-18Mn-0.8 C-0.2 V TWIP steel. *Mater. Res. Expr.* **2020**, *6*, 1265h4. [CrossRef]
14. Han, G.M.; Tian, C.G.; Chu, Z.K.; Cui, C.Y.; Hu, Z.Q.; Sun, X.F. Activation energy calculations for the Portevin–Le Chatelier effect in nimonic 263 superalloy. *Met. Mater. Trans. A* **2015**, *46*, 4629–4635. [CrossRef]
15. Yong, Q. *Secondary Phase in Steels*; Press of Metallurgy Industry: Beijing, China, 2006.
16. Sun, S.; Xue, Z.; An, L.; Chen, X.; Liu, Y. A novel design to enhance the mechanical properties in Cu-Bearing antibacterial stainless steel. *Materials* **2020**, *13*, 403. [CrossRef]
17. Shen, Y.F.; Jia, N.; Misra, R.D.K.; Zuo, L. Softening behavior by excessive twinning and adiabatic heating at high strain rate in a Fe–20Mn–0.6 C TWIP steel. *Acta Mater.* **2016**, *103*, 229–242. [CrossRef]
18. Bintu, A.; Vincze, G.; Picu, C.R.; Lopes, A.B.; Grácio, J.J.; Barlat, F. Strain hardening rate sensitivity and strain rate sensitivity in TWIP steels. *Mater. Sci. Eng. A* **2015**, *629*, 54–59. [CrossRef]
19. Curtze, S.; Kuokkala, V. Dependence of tensile deformation behavior of TWIP steels on stacking fault energy, temperature and strain rate. *Acta Mater.* **2010**, *58*, 5129–5141. [CrossRef]
20. Yang, H.K.; Zhang, Z.J.; Dong, F.Y.; Duan, Q.Q.; Zhang, Z.F. Strain rate effects on tensile deformation behaviors for Fe–22Mn–0.6C–(1.5Al) twinning-Induced plasticity steel. *Mater. Sci. Eng. A* **2014**, *607*, 551–558. [CrossRef]
21. Chen, L.; Kim, H.S.; Kim, S.K. Localized deformation due to Portevin–LeChatelier effect in 18Mn–0.6 C TWIP austenitic steel. *ISIJ Int.* **2007**, *47*, 1804–1812. [CrossRef]
22. Yoshinaga, H.; Morozumi, S. A Portevin-Le Chatelier effect expected from solute atmosphere dragging. *Philos. Mag. A J. Theor. Exp. Appl. Phys.* **1971**, *186*, 1351–1366. [CrossRef]
23. Qian, K.; Li, X.; Xiao, L.; Chen, W.; Zhang, H.; Peng, K. Dynamic strain aging phenomenon in metals and alloys. *J. Fuzhou Univ. (Nat. Sci. Ed.)* **2001**, *6*, 8–23.
24. Kawakami, K.; Matsumiya, T. Numerical analysis of hydrogen trap state by TiC and V4C3 in bcc-Fe. *ISIJ Int.* **2012**, *52*, 1693–1697. [CrossRef]
25. Hu, G.; Wang, X.; Rong, Y. *Fundamentals of Materials Science*; Shanghai Jiao Tong University Press: Shanghai, China, 2010.